ACS OMEGA

http://pubs.acs.org/journal/acsodf

Article

Isoindolin-1-ones Fused to Barbiturates: From Design and Molecular Docking to Synthesis and Urease Inhibitory Evaluation

Houman Kazemzadeh, Elham Hamidian, Faezeh Sadat Hosseini, Movahed Abdi, Fatemeh Niasari Naslaji, Meysam Talebi, Mehdi Asadi, Mahmood Biglar, Issa Zarei, and Massoud Amanlou*

Cite This: *ACS Omega* 2022, 7, 19401−19411

Read Online

ACCESS | Metrics & More | Article Recommendations | Supporting Information

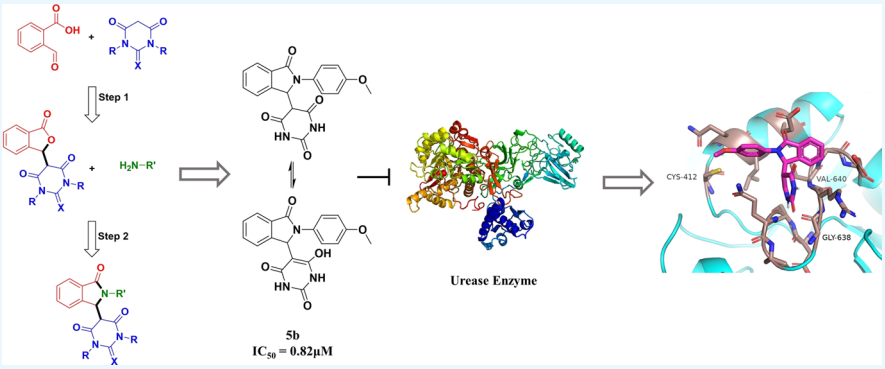

ABSTRACT: *Helicobacter pylori*-induced ulcers and gastric cancer have been one of the main obstacles that the human community has ever struggled with, especially in recent decades. Several different attempts have been made to eradicate this group. One of the most widely used attempts is to inhibit the critical enzyme that facilitates its survival, the urease enzyme. Therefore, in this study, isoindolin-1-ones fused to barbiturates were designed, synthesized, and evaluated for their in vitro urease inhibitory activity as novel inhibitors for the urease enzyme. The synthesis route consisted of two steps. These steps increased the yield rate and decreased the percentage of byproducts while approaching green chemistry using ethanol and water as green solvents and microwave irradiation instead of conventional methods. In vitro urease inhibitory results indicated that all the compounds had higher inhibitory activity than the standard inhibitor, thiourea, and compound **5b** proved to be the most potent inhibitor (IC_{50} = 0.82 ± 0.03 μM). A molecular docking study was performed to understand the interaction between compounds **5a−n** and Jack bean urease enzyme. The results of the molecular docking study were also in harmony with the in vitro results, which are discussed in detail later in this study.

1. INTRODUCTION

Gastric cancer has been harassing human health by taking the lives of 783,000 individuals every year.[1] Risk factors play a major role in this disaster. These factors vary from infectious diseases to inappropriate life habits.[2] Identifying and controlling these factors can prevent the progression of this cancerous disease. The well-known infectious factor for gastric cancer is proved to be *Helicobacter pylori* (*H. pylori*).[3] *H. pylori* is a spiral-shaped bacillus that lives in the stomach. The flagella enable the bacterium to move from the acidic medium to the mucus layer, where the pH is higher. Also, it can attach to the epithelium surface and escape the two major defensive barriers of the stomach.[4] Furthermore, it has a unique urease enzyme. The urease enzyme is present in many groups of bacteria,[5] including those that cause kidney stones.[6] Still, this enzyme hydrolyzes the urea in the gastrointestinal juice to ammonia and carbon dioxide in the stomach. Ammonia neutralizes the acidic pH and assists the bacterium's survival.[7] The mentioned survival mechanisms allow *H. pylori* to breed and harm gastric lining cells. This harm can cause peptic and duodenal ulcers in the short term and chronic inflammation and gastric cancer in the long term.[8]

Numerous attempts have been made to design new drugs with multiple mechanisms to eradicate this group of bacteria and prevent the progression of *Helicobacter pylori*-induced gastric cancer. One of these attempts is to inhibit the urease enzyme for the purpose of preventing the escape from acidic pH.[9] Several chemicals have been introduced as urease inhibitors, including hydroxamic acids, phosphoramidates,

Received: February 23, 2022
Accepted: May 18, 2022
Published: June 2, 2022

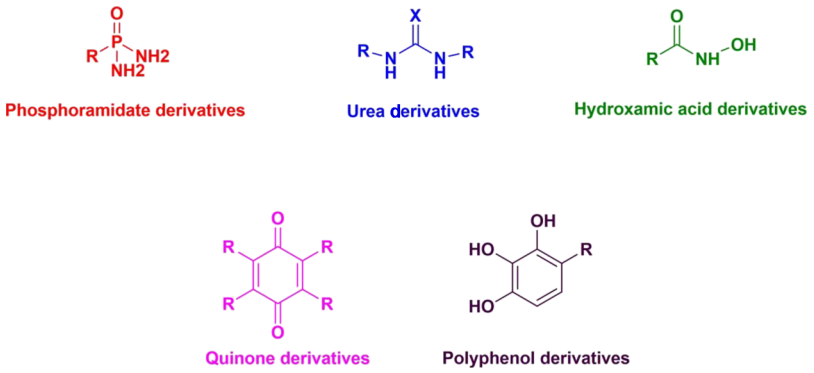

Figure 1. General structure for some novel urease inhibitors in the literature.

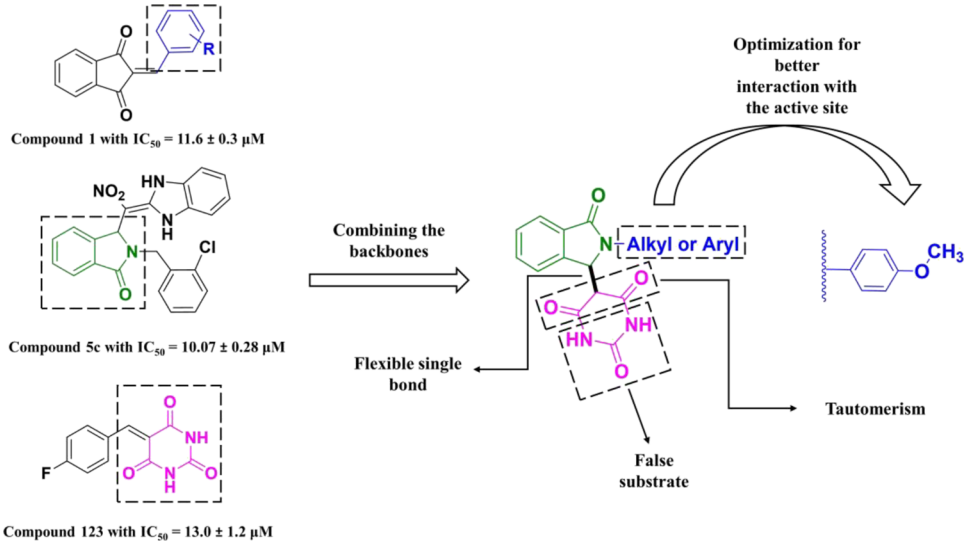

Figure 2. Principles behind the design of novel urease inhibitors bearing barbiturate and isoindolin-1-one in their structure.

urea derivatives, quinones, polyphenols, and so forth (Figure 1).[10] By interacting with the enzyme, these chemicals prevent the decomposition of urea, and therefore, without ammonia, the bacterium will not be able to survive in the stomach's acidic medium. Despite the vast number of urease inhibitors, because of the high capability of *H. pylori* to resist against many types of chemicals that can ruin its specialized features including the urease enzyme, ongoing drug designs, synthesis, and biological and clinical studies are needed to achieve the optimum structure for urease inhibition.

From previous studies, it is well recognized that barbiturates, thiobarbiturates, and 1,3 dimethyl barbiturates are potential candidates for urease inhibition,[11−13] even though they have many other potent pharmacological effects.[14] Furthermore, urease inhibitory activity of different isoindolin-1-one derivatives was also reported.[15] Therefore, in this article, based on the mentioned studies and our computer-aided calculations, novel isoindolin-1-one derivatives that are fused to different barbiturates were designed and synthesized. Then, the urease inhibitory activity of the synthesized compounds was evaluated. The results revealed the high inhibitory activity of these derivatives against the enzyme above, with a half-maximal inhibitory concentration (IC_{50}) ranging from 0.82 to 1.85 μM.

2. RESULTS AND DISCUSSION

2.1. Design. Throughout the years, drug design and discovery methods have evolved tremendously. This evolution is a debtor to the rapid development of computer technology and bioinformatics, which has enabled scientists to lower costs, better understand ligand-receptor interactions, and appropriately predict the pharmacokinetics and pharmacodynamics before clinical evaluation.[16] These new drug discovery methods are categorized into two major groups: structure-based and ligand-based drug discovery.[17] Each of them uses their unique strategies to discover new drugs. For instance, in the structure-based drug design, which also applies to our research, molecular docking, molecular dynamic simulation, and virtual screening are exploited. In contrast, techniques like pharmacophore modeling, quantitative structure−activity relationships (QSARs), and artificial intelligence (AI) are applied in the ligand-based drug design. Therefore, in this study, the general structure from previous studies was considered to get the most out of it and achieve an optimum structure. As mentioned in the Introduction, urea derivatives are among the most widely used backbones to discover urease inhibitors. Barbiturates are a significant group that bear a urea backbone in their structure. They act as a false substrate in the active site and interrupt enzyme activity.[18] Introducing different moieties to their structure can improve their ability to fill the active site by interacting with essential residues. They

https://doi.org/10.1021/acsomega.2c01028
ACS Omega 2022, 7, 19401−19411

Scheme 1. Schematic Representation of the Two Steps of the Synthesis

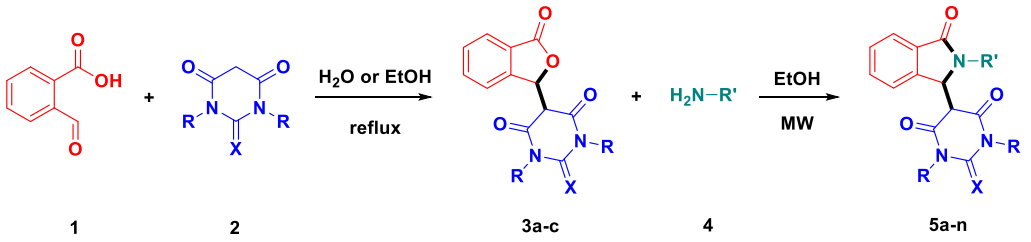

Scheme 2. Proposed Mechanism for the First Step of the Synthesis

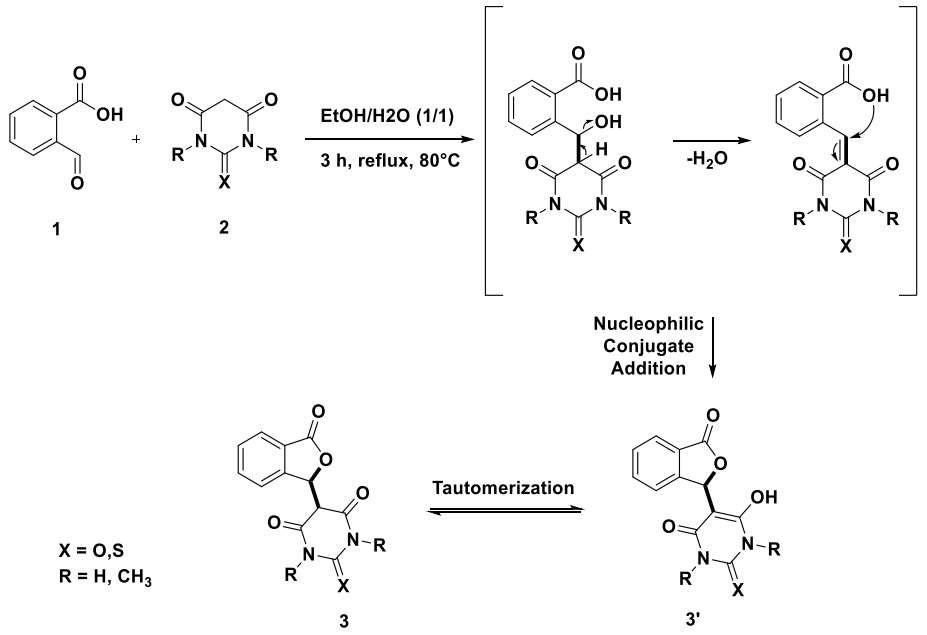

can also interact with the active site's nickel atoms, but it is not mandatory for the inhibition. The introduced moieties in the literature include triazoles,[12] aryl groups,[11] phenyl acetamide on nitrogen,[11] amines and anilines,[19] hydrazine,[13] pyridine,[20] and so forth. They demonstrated a wide range of urease inhibitory activity. Other inhibitors that proved their urease inhibitory activity are compounds with isoindolin-1-one building blocks.[15] In addition to their vast range of pharmacologic effects,[21] they also demonstrated acceptable urease inhibition and interacted with the key residues and nickel ions in the active site. The isoindolin-1-one part also interacted with the key residues in the active site.

Therefore, by considering the data collected from barbiturate and isoindolin-1-one derivatives,[15,22] these two backbones were attached in a way that could be synthetically feasible and also have practical orientation in the active site. At first, these two were linked with a single bond to increase barbiturate flexibility in the active site for better fitting. After that, tautomerism was considered as an enabling tool for our inhibitors. Different conformations could be achieved by the movement of hydrogen, and therefore, the interaction with the active site could be improved. For the third part of our design, inhibitors similar to our new backbone were investigated.[23] As shown in Figure 2, different alkyl and aryl groups were used. While considering the three-dimensional (3D) structure of our inhibitors, the barbiturate and isoindolin-1-one parts are perpendicular to each other. Therefore, when they reach the active site, they anchor on it. For barbiturates to have better competition with urea, the isoindolin-1-one part should stabilize the whole structure in the active site. Therefore, by conducting a molecular docking study, the results indicated that introducing aryl groups better stabilizes the inhibitor. Similar to the result of benzylidine indane-1,3-diones-based inhibitors, the para methoxyphenyl group better stabilized and inhibited the urease enzyme.

Eventually, to confirm all these, a molecular docking study was performed. As the results show in the corresponding section, the compounds fit in the active site in a fashion similar to other mentioned inhibitors and can inhibit the activity of the urease enzyme.

2.2. Chemistry. In this article, 14 novel compounds with high urease inhibitory activity were synthesized according to Scheme 1. In the first step, 2-formyl benzoic acid **1** was reacted with barbiturate derivatives **2** in water or 50% ethanol as the solvent to get compounds **3a−c**. The yield of the first step was between 70 and 88%.[24,25] At first, a Knoevenagel reaction occurs between the aldehyde group of 2-formyl benzoic acid **1** and barbiturate derivatives **2**. This leads to forming a double bond conjugated to the carbonyl groups of the barbiturates **2**. Then, nucleophilic conjugate addition occurs between the oxygen group and the conjugated double bond, the lactone ring is created, and the final structure of the intermediates is formed (Scheme 2).

In the second step, a mixture of **3a−c** and different aromatic/aliphatic amines **4** in ethanol as the solvent was subjected to microwave irradiation to obtain compounds **5a−**

https://doi.org/10.1021/acsomega.2c01028
ACS Omega 2022, 7, 19401−19411

Scheme 3. Proposed Mechanism for the Second Step of the Synthesis

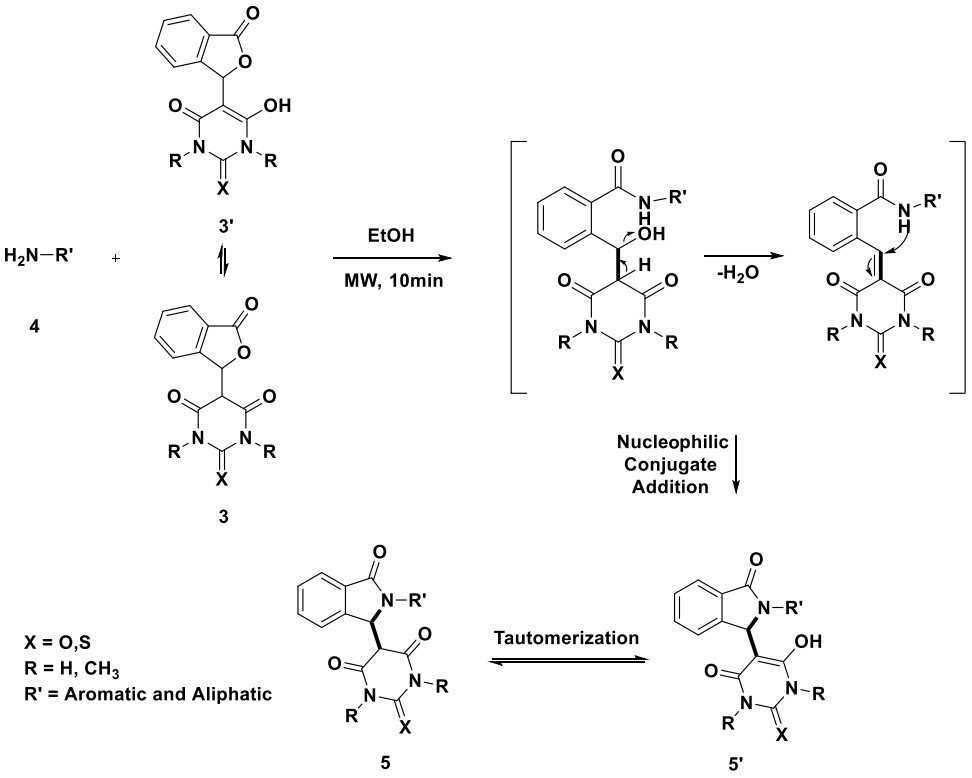

n. The yield of the second step was between 25 and 95%. At first, an aminolysis reaction occurs between the aromatic/aliphatic amines **4** and the intermediates **3**. An amide bond is formed, and the negatively charged oxygen receives a hydrogen atom and becomes a hydroxy group. Then, by eliminating water, a conjugated double bond is created. The amide group attacks the conjugated double bond via nucleophilic conjugate addition, the lactam ring is formed, and the final isoindolin-1-one structure is obtained (Scheme 3). Final compound structures were confirmed using mass, ^{1}H NMR, and ^{13}C NMR spectroscopy.

2.3. Urease Inhibitory Activity of Compounds 5a−n.

All the synthesized compounds were evaluated for their inhibitory activity against jack bean urease. The results indicated that all the compounds, **5a−n**, were at least 12 times to a maximum of 27 times more potent than the standard inhibitor, thiourea (Table 1 and Figure 3). Compound **5b** was the most potent inhibitor (IC_{50} = 0.82 ± 0.03 μM). The structural analysis concluded that introducing a substituted phenyl moiety on the nitrogen of isoindolin-1-one enhances the biological activity. Furthermore, the bulkier the groups get at the meta and para positions, especially in the para position, the more potent the inhibition. This may be because, in those positions, there is a hydrophobic pocket that interacts better with bulkier groups. In the case of compound **5b**, which bears an o-methoxy group in the para position, a weak hydrogenic bond was formed between the oxygen atom and Cys 412 that is not present in the other compounds. This interaction can be the possible explanation for the higher activity of compound **5b**.

The effect of different barbiturate derivatives on the whole inhibitory activity of compounds was also studied. The results suggested that compounds with the barbiturate moiety were more potent than those with 1,3-dimethyl barbiturate and thiobarbiturate. Moreover, based on the obtained results, compounds with the 1,3-dimethyl barbiturate moiety demonstrated higher activity than those with thiobarbiturate.

Table 1. Urease Inhibitory Activity of Isoindolin-1-one-Synthesized Compounds

compound	IC_{50} ± SEM[a] (μM)
5a	1.85 ± 0.06
5b	0.82 ± 0.03
5c	1.25 ± 0.05
5d	1.07 ± 0.02
5e	0.96 ± 0.01
5f	0.96 ± 0.01
5g	1.09 ± 0.07
5h	1.28 ± 0.04
5i	1.22 ± 0.05
5j	1.78 ± 0.10
5k	1.62 ± 0.05
5l	1.85 ± 0.06
5m	0.97 ± 0.01
5n	1.34 ± 0.01
thiourea[b]	22 ± 1.2

[a]SEM (standard error mean). [b]Thiourea (standard inhibitor).

On a final note, compound **5b** possesses all the mentioned features in this section to achieve the optimum inhibitor. Like many other candidates, this is only a model-based examination of the activity of compound **5b** in the laboratory. To achieve an optimum inhibitor, further experimental investigations, including cytotoxicity evaluation against human cells, microbiological tests against *H. pylori*, animal model tests, and after passing all the mentioned evaluations, clinical trials are required to be carried out to establish whether this compound has high urease activity in mentioned cases. Compound **5b** can

https://doi.org/10.1021/acsomega.2c01028
ACS Omega 2022, 7, 19401−19411

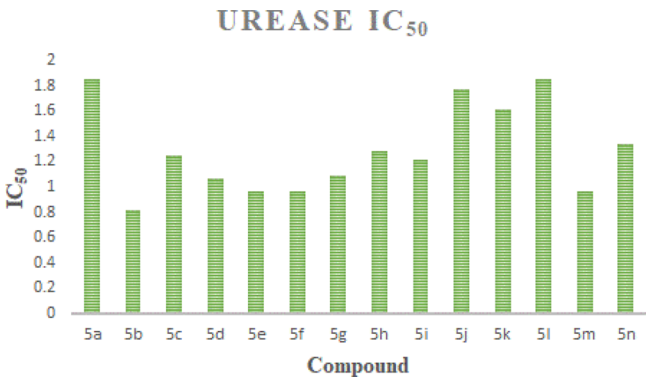

Figure 3. Graphical representation of IC_{50} values for compounds **5a–n**.

also be used as a lead compound for future drug design and discovery.

2.4. Docking Study. To understand the possible interactions between the synthesized compounds and the active site of the Jack bean urease enzyme, molecular docking simulations were performed. The results (Table 2) indicated that all compounds interacted well with the active site. Minimum binding energies ranged between −7.14 and −5.77 kcal/mol, which was more potent than the standard inhibitor, thiourea. The superimposed illustration of each compound's best docking pose in the enzyme's active site is shown in Figure 4. While the results of the docking study reveal that compound **5e** has the lowest binding energy, the in vitro results confirm that compound **5e** is our second most potent inhibitor after compound **5b**. This discrepancy can be attributed to several factors. These factors include:[26−28]

- Desolvation effects and entropy disturb docking scoring functions.
- Docking accuracy has fluctuated from 0 to 92.66% in some cases since it is based on algorithms and scoring functions.
- Molecular docking only provides calculated binding affinity and represents the protein selectivity for a specific ligand. In real-world data, factors like the concentration of the enzyme, the assay conditions, the mechanism of inhibition, the concentration of inhibitor in the active site, and so forth affect the IC_{50} results.
- The strong binders in the docking study are the best predicted spatial orientation of a ligand in the active site, and they may not be the biologically active conformer.
- IC_{50} gives you the amount needed for inhibition, while docking only gives you the required amount for binding. That is why docking cannot predict if the binding ligand inhibits the enzyme or not.
- As shown in Figure 4, compound **5b** forms three hydrogen bonds with the active site, whereas compound **5e** only forms one. For this reason, compound **5b** creates a more stable interaction with the active site and spends more time in the active site before dissociating from it.

Therefore, based on the factors mentioned above and the biological assay results, the interaction between compound **5b** and the enzyme's active site will be surveyed. This compound forms three hydrogen bonds with Gly 638, Val 640, and Cys

Table 2. Physicochemical Properties and the Docking Results of Isoindolin-1-one-Synthesized Compounds

compound	lowest binding energy (kcal/mol)	H bond acceptor	H bond donor	TPSA (Å^2)	MW (g/mol)	MlogP	Lipinski	esol class
5a keto	−6.85	4	2	95.58	335.31	1.50	yes	soluble
5a enol	−6.49	4	3	106.26	335.31	2.03	yes	soluble
5g keto	−6.77	4	2	95.58	349.34	1.73	yes	soluble
5g enol	−6.71	4	3	106.26	349.34	2.26	yes	soluble
5d keto	−7.01	4	2	95.58	363.37	1.96	yes	soluble
5d enol	−6.32	4	3	106.26	363.37	2.49	yes	soluble
5b keto	−6.66	5	2	104.81	365.34	1.21	yes	soluble
5b enol	−6.48	5	3	115.49	365.34	1.74	yes	soluble
5h keto	−6.82	5	2	95.58	353.30	1.88	yes	soluble
5h enol	−6.79	5	3	106.26	353.30	2.41	yes	soluble
5c keto	−6.79	4	2	95.58	369.76	2.00	yes	soluble
5c enol	−6.58	4	3	106.26	369.76	2.53	yes	soluble
5e keto	−7.14	4	2	95.58	414.21	2.11	yes	soluble
5e enol	−6.91	4	3	106.26	414.21	2.64	yes	soluble
5f keto	−6.78	4	2	95.58	404.20	2.50	yes	moderately soluble
5f enol	−6.65	4	3	106.26	404.20	3.03	yes	moderately soluble
5i keto	−6.63	4	2	95.58	369.76	2.00	yes	soluble
5i enol	−6.34	4	3	106.26	369.76	2.53	yes	soluble
5j keto	−6.73	4	2	95.58	404.20	2.50	yes	soluble
5j enol	−6.39	4	3	106.26	404.20	3.03	yes	soluble
5k keto	−6.1	4	2	95.58	315.32	0.98	yes	soluble
5k enol	−5.98	4	3	106.26	315.32	1.50	yes	soluble
5l ketone	−5.77	4	2	95.58	301.3	0.73	yes	soluble
5l enol	−5.77	4	3	106.26	301.3	1.25	yes	soluble
5m ketone	−6.5	5	0	87.23	393.39	1.66	yes	soluble
5m enol	−6.76	5	1	93.77	393.39	2.19	yes	soluble
5n ketone	−6.85	4	2	119.83	381.41	1.19	yes	soluble
5n enol	−6.74	4	3	130.51	381.41	1.72	yes	soluble

https://doi.org/10.1021/acsomega.2c01028
ACS Omega 2022, 7, 19401−19411

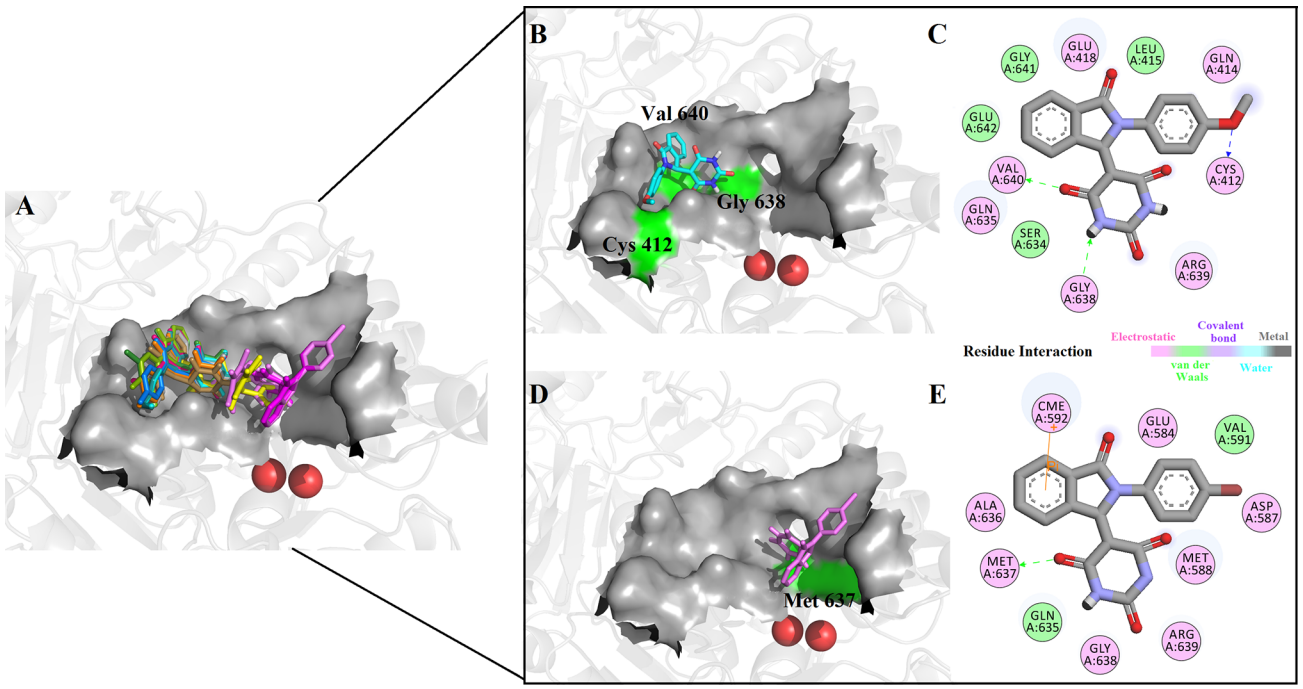

Figure 4. A. Superimposed picture of the best docking pose of each compound in the active site of the enzyme. B and C: 3D and 2D illustration of the interaction of compound **5b** in the enzyme's active site. D and E: 3D and 2D images of the interaction of compound **5e** in the enzyme's active site.

412 and several different π bonds with Gln 414, Leu 415, Glu 418, Ser 634, Gln 635, Arg 639, Gly 641, and Glu 642 (Figure 4). These interactions intercept the entrance of the substrate into the active site, and thus, the urease enzyme activity is strongly inhibited.

Moreover, to understand the ADME properties of the compounds **5a−n**, the SwissADME webserver was utilized, and Lipinski's rule of five was used to ascertain if the synthesized compounds have suitable druglike features.[29,30] The results indicated that compounds **5a−n**, either in the keto form or in the enol form, obeyed all the rules in Lipinski's rule of five without any violation. Their calculated solubility was in an acceptable range. The results of Compound **5b**, the best compound from the in vitro results, were as follows: molecular weight of 400.38 g/mol, LogP 1.21 for the keto form and 1.74 for the enol form, two hydrogen bond donors in the keto form, three hydrogen bond donors in the enol form, and five hydrogen bond acceptors in both forms.

3. CONCLUSIONS

Based on previous research, this study aimed to design inhibitors with both isoindolin-1-one and barbiturate moiety in their structure. The prepared compounds were synthesized in two steps. Both steps were in good yields. The inhibition capability of compounds was evaluated against jack bean urease. The results indicated a remarkably higher inhibitory activity of compounds than the standard inhibitor, thiourea. The molecular docking study confirmed the results obtained from the biological examination. Reasonable interactions between the active site of the enzyme and synthesized compounds is demonstrated. Compound **5b** proved itself as the most potent inhibitor, confirmed by both docking and biological study. While bearing compound **5b** in mind, novel compounds carrying the isoindolin-1-one and barbiturate structure can be a good backbone for designing and synthesizing new urease inhibitors.

4. MATERIALS AND METHODS

4.1. General Information. All chemicals and solvents used in this study were purchased from Merck and used without further purification. ^{1}H NMR and ^{13}C NMR were recorded on a Bruker FT-500 using $CDCl_3$ or dimethylsulfoxide (DMSO) as the solvent and tetramethylsilane (TMS) as the internal standard. Analytical thin layer chromatography was used for exploring the reaction progression. Melting points were obtained using a Kofler hot stage apparatus. Mass spectra were obtained with an HP (Agilent technologies) 5937 mass selective detector (USA). Microwave reactions were performed using modified Samsung SmartSensor Microwave − ME6144ST (maximum output power 1000 W, Teflon-coated magnetic stir bar, temperature range 40−200 °C). Liquid chromatography−mass spectrometry (LC−MS) results were obtained using SCIEX Triple Quad 5500 Plus LC−MS/MS System − QTRAP Ready. The MS source conditions were set as follows: GS1 flow, 55 L/min; GS2 flow, 55 L/min; curtain gas (CUR) flow, 20 L/min; ion spray voltage of MS, −4500 V. MS data were collected using the Analyst 1.7.2 software.

4.2. Chemistry. *4.2.1. General Procedure for the Synthesis of 5-(3-Oxo-1,3-dihydroisobenzofuran-1-yl) Barbituric Acid (**3a**)/5-(3-Oxo-1,3-dihydroisobenzofuran-1-yl)-2-thiobarbituric Acid (**3c**).* To a mixture of barbituric acid (**2a**)/thiobarbituric acid (**2c**) (10 mmol) in 50% ethanol (20 mL), 2-formyl benzoic acid (**1**) (10 mmol) was added. The mixture was heated to 80 °C and refluxed for 3 h. After completing the reaction, the mixture was cooled, the precipitate was filtered off, washed with cold water and ethanol, and recrystallized from ethanol.[24]

4.2.2. General Procedure for the Synthesis of 1,3-Dimethyl-5-(3-oxo-1,3-dihydroisobenzofuran-1-yl) Barbitu-

https://doi.org/10.1021/acsomega.2c01028
ACS Omega 2022, 7, 19401−19411

*ric Acid (**3b**).* To a mixture of 1,3-dimethyl barbituric acid (**2b**) (10 mmol) in water (20 mL), 2-formyl benzoic acid (**1**) (10 mmol) was added. The mixture was stirred for 3 h at room temperature. After completing the reaction, the precipitate was filtered off and washed with cold water and ethanol[25] (Scheme 2).

*4.2.3. General Procedure for the Synthesis of Final Derivatives (**5a−n**).* The mixture of **3** (1 mmol) and different derivatives of aniline and alkyl amines (isopropyl and isobutyl) (**4**) (1 mmol) in 3 mL of ethanol was subjected to microwave irradiation for 10 min. After completing the reaction, the precipitate was filtered off and washed with cold water to obtain the product (Table 3). In the case of compounds **5b** and **5n**, ethanol was removed in vacuo to obtain the product (Scheme 3).

Table 3. General Structure of the Intermediates (3a−c) and the Final Products (5a−n)

compound	X	R	R′
3a	O	H	
3b	O	CH_3	
3c	S	H	
5a	O	H	phenyl
5b	O	H	4-methoxy phenyl
5c	O	H	4-chlorophenyl
5d	O	H	3,4-dimethyl phenyl
5e	O	H	4-bromo phenyl
5f	O	H	3,4-dichloro phenyl
5g	O	H	4-methyl phenyl
5h	O	H	4-fluoro phenyl
5i	O	H	3-chlorophenyl
5j	O	H	3,5-dichloro phenyl
5k	O	H	isobutyl
5l	O	H	isopropyl
5m	O	CH_3	4-methoxy phenyl
5n	S	H	4-methoxy phenyl

4.2.4. Tautomerism in the Barbiturate Region. As can be seen in Scheme 4, the titled compounds have tautomerism in their barbiturate region. Usually, barbituric acids exist primarily in the keto form.[31] For instance, in DMSO, barbituric acid is only 2−3% enolized,[32] but when it is substituted at the 5′ position, its enolizability is altered. This alteration can be due to many factors. These factors include change in the CH acidity after introducing substitutes at the 5′ position, which is closely related to the enolizability, especially in *trans* fixed *β*-diketones,[33,34] the polarity of the solvent,[32] electronic and steric effects of the substitutes at the 5′ position,[35] change in the interaction path of the CH group and the imino group with the solvent after the presence of the substitutes at the 5′ position,[36] change in the internal interaction,[35] and so forth. The net effect of all these factors causes a shift in the tautomer conversion rate and allows us to observe tautomerism in NMR spectra. Tautomerism affects NMR spectra so that the two major tautomeric forms with relatively low conversion rates show different but overlapped NMR spectra.[35] Assigning the peaks to their corresponding tautomeric form can be done by considering the multiplicity and chemical shift of the signals, even though tautomerism disturbs many factors in NMR spectra, like bringing extra signals and causing error in the integration value.[37]

Scheme 4. Tautomerism in the Barbiturate Region of Compounds 3a−c and 5a−n

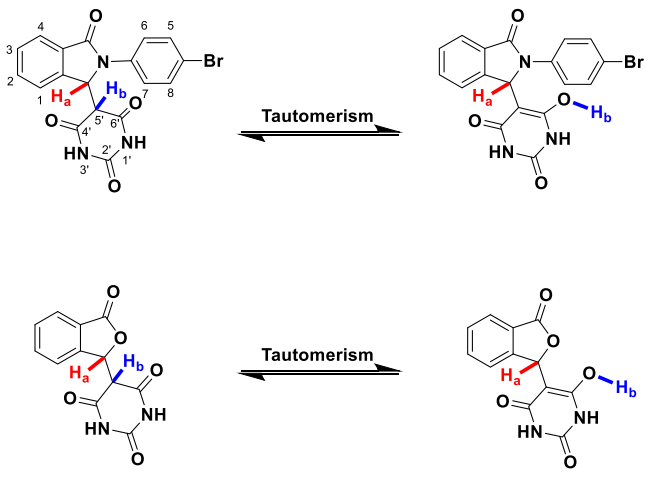

Furthermore, when two independent and nonoverlapped peaks corresponding to each tautomer are detected in ^{1}H NMR spectra, their integration calculates the ratio between two tautomeric forms.[38] In our case, both H_a and H_b can be used to calculate the keto/enol ratio. The problem with H_b is that it could not be detected in the enol form in ^{1}H NMR spectra. Therefore, H_a was used for the keto/enol ratio calculation.

The main issue with the integration values is that they have a typical error of 5%. When tautomerism occurs, the picks overlap, extra signals emerge, and their integration value can demonstrate a higher error percentage.[35,39] Therefore, these issues make NMR spectra, even more, complicated.[39−41] Numerous methods have been used to overcome tautomerism and limit the structure to only one tautomeric form. These methods include changing the solvent, increasing or decreasing the temperature, increasing or decreasing the concentration of compounds, using specialized chemicals, and so forth.[42]

Because of the lack of access to almost all of the mentioned methods and solubility problems of our compounds, which are only soluble in DMSO, except for compound **3b**, which is soluble in $CHCl_3$, we can only report the ^{1}H NMR and ^{13}C NMR spectra in DMSO and the tautomeric ratio between the keto and the enol form in DMSO at 25 °C. The percentage of the enol form can be calculated using this equation:[35,38,43] % Enol = [(the integration value of H_a in the enol form)/(the integration value of H_a in the enol form + the integration value of H_a in the keto form)] *100. The percentage of the keto form can be calculated from this equation:

$$\%\text{Keto} = 100 - \%\text{Enol}$$

*4.2.4.1. 5-(3-Oxo-1,3-dihydroisobenzofuran-1-yl) Barbituric Acid (**3a**).* Yellow powder; yield: 88%; mp: 305 °C; ^{1}H NMR (500 MHz, DMSO-d_6) *δ*: 11.59 (s, 1H, NH Keto), 11.36 (s, 1H, NH Keto), 10.95 (s, 2H, 2 × NH Enol), 8.16−7.18 (m, 8H + H_a Enol), 6.24 (s, 1H, H_a Keto), 4.65 (s, 1H, H_b Keto); ^{13}C NMR (125 MHz, DMSO-d6); *δ* 181.88, 169.78, 162.62, 150.82, 150.79, 134.76, 129.35, 125.19, 123.15, 78.94, 51.12; MS (*m*/*z*, %): 260.1 (M^+, 13), 231.1 (100), 215.1,[44] 133.1 (81), 104.1 (62), 77.1;[36] Tautomeric form (%): 40 Enol.

*4.2.4.2. 1,3-Dimethyl-5-(3-oxo-1,3-dihydroisobenzofuran-1-yl) Barbituric Acid (**3b**).* White powder; yield: 95%; mp: 185 °C; ^{1}H NMR (500 MHz, $CHCl_3$) *δ*: 7.91 (d, *J* = 7.7 Hz, 1H,

https://doi.org/10.1021/acsomega.2c01028
ACS Omega 2022, 7, 19401−19411

H_4), 7.75 (t, J = 7.6 Hz, 1H, H_2), 7.60 (t, J = 7.5 Hz, 1H, H_3), 7.55 (d, J = 7.7 Hz, 1H, H_1), 6.27 (s, 1H, H_a Keto), 4.12 (s, 1H, H_b Keto), 3.35 (s, 3H, NCH_3 Keto), 3.18 (s, 3H, NCH_3 Keto); ^{13}C NMR (125 MHz, $CDCl_3$) δ: 169.08, 165.66, 163.45, 150.83, 146.75, 134.55, 129.88, 126.03, 125.89, 121.73, 79.15, 51.60, 29.00, 28.63; MS (m/z, %): 288.1 (M^+, 6), 259.2 (100), 133.1 (63), 104.1,[34] 77.1;[22] Tautomeric form (%): 0 Enol.

*4.2.4.3. 5-(3-Oxo-1,3-dihydroisobenzofuran-1-yl)-2-thiobarbituric Acid (**3c**).* Yellow powder; yield: 70%; mp: 250 °C; ^{1}H NMR (500 MHz, DMSO-d_6) δ: 11.83 (s, 2H, 2 × NH Enol), 7.77 (d, J = 7.5 Hz, 1H, H_4), 7.64 (t, J = 7.5 Hz, 1H, H_2), 7.49 (t, J = 7.5 Hz, 1H, H_3), 7.42 (d, J = 7.8 Hz, 1H, H_1), 6.67 (s, 1H, H_a Enol). ^{13}C NMR (125 MHz, DMSO-d_6) δ: 175.36, 170.66, 161.54, 149.52, 134.04, 128.85, 127.26, 125.02, 122.86, 100.92, 94.24, 74.86; MS (m/z, %): 276.1 (M^+, 24), 247.1,[15] 231.1,[22] 133.1 (100), 105.1,[17] 77.1;[17] Tautomeric form (%): 100 Enol.

*4.2.4.4. 5-(3-Oxo-2-phenylisoindolin-1-yl) Barbituric Acid (**5a**).* White powder; yield: 79%; mp: 260−262 °C; ^{1}H NMR (500 MHz, DMSO-d_6) δ: 11.54 (s, 2H, 2 × NH Keto), 11.02 (s, 2H, 2 × NH Enol), 7.99−6.71 (m, 18H, aromatic), 6.33 (s, 1H, H_a Enol), 6.14 (s, 1H, H_a Keto), 4.08 (s, 1H, H_b Keto). ^{13}C NMR (125 MHz, DMSO-d_6) δ: 172.57, 167.38, 164.64, 162.66, 151.68, 147.48, 141.07, 138.87, 133.03, 132.04, 129.76, 129.57, 128.60, 127.55, 125.06, 123.99, 122.83, 122.41, 122.41, 122.10, 118.79, 82.58, 57.50; MS (m/z, %): 335.1 (M^+, 9), 208.1 (100), 93.1,[16] 77.1 (55), 51.1,[20] 42.1;[20] LC−MS (negative ion mode): m/z 334 $(M-H)^-$ for $C_{18}H_{13}N_3O_4$; Purity (%): 98.83; Tautomeric form (%): 63 Enol.

*4.2.4.5. 5-(2-(4-Methoxyphenyl)-3-oxoisoindolin-1-yl) Barbituric Acid (**5b**).* Light green powder; yield: 71%; mp: 158−160 °C; ^{1}H NMR (500 MHz, DMSO-d_6) δ: 11.49 (s, 2H, 2 × NH Keto), 11.01 (s, 2H, 2 × NH Enol), 7.89−6.74 (m, 16H, aromatic), 6.28 (s, 1H, H_a Enol), 6.02 (s, 1H, H_a Keto), 4.06 (s, 1H, H_b Keto), 3.83−3.71 (m, 6H, 2 × OCH_3 Keto and Enol); ^{13}C NMR (125 MHz, DMSO-d_6) δ: 172.52, 167.47, 159.15, 158.06, 132.73, 129.44, 127.22, 124.67, 124.28, 123.74, 122.29, 115.37, 114.65, 114.02, 61.43, 57.19, 55.93, 55.80, 48.68; MS (m/z, %): 365.2 (M^+, 20), 238.2 (100), 231.1,[27] 133.1,[40] 108.1;[28] LC−MS (negative ion mode): m/z 364.01 $(M-H)^-$ for $C_{19}H_{15}N_3O_5$; Purity (%): 98.80; Tautomeric form (%): 35 Enol.

*4.2.4.6. 5-(2-(4-Chlorophenyl)-3-oxoisoindolin-1-yl) Barbituric Acid (**5c**).* White powder; yield: 30%; mp: 275−280 °C; ^{1}H NMR (500 MHz, DMSO-d_6) δ: 11.59 (s, 2H, 2 × NH Keto), 11.08 (s, 2H, 2 × NH Enol), 7.94−6.61 (m, 16H, aromatic), 6.32 (s, 1H, H_a Enol), 6.15 (s, 1H, H_a Keto), 4.10 (s, 1H, H_b Keto); ^{13}C NMR (125 MHz, DMSO-d_6) δ: 167.41, 164.09, 151.17, 143.70, 132.40, 129.30, 128.65, 126.49, 123.61, 122.90, 122.53, 118.32, 57.12; MS (m/z: %): 369.1 (M^+, 8), 242.1 (100), 127.1 (66), 65.1;[20] LC−MS (negative ion mode): m/z 367.91 $(M-H)^-$ for $C_{18}H_{12}ClN_3O_4$; Purity (%): 96.44; Tautomeric form (%): 62 Enol.

*4.2.4.7. 5-(2-(3,4-Dimethylphenyl)-3-oxoisoindolin-1-yl) Barbituric Acid (**5d**).* Yellow powder; yield: 40%; mp: 240−245 °C; ^{1}H NMR (500 MHz, DMSO-d_6) δ: 11.54 (s, 2H, 2 × NH Keto), 11.02 (s, 2H, 2 × NH Enol), 7.94−6.78 (m, 14H, aromatic), 6.28 (s, 1H, H_a Enol), 6.04 (s, 1H, H_a Keto), 4.07 (s, 1H, H_b Keto), 2.31−2.11 (m, 12H, 4 × CH_3 Keto and Enol); ^{13}C NMR (125 MHz, DMSO-d6) δ: 166.68, 164.67, 147.49, 138.17, 136.02, 134.75, 131.88, 130.87, 129.50, 127.42, 123.58, 122.95, 122.33, 119.68, 119.40, 82.65, 57.54, 20.14, 19.84, 19.28; MS (m/z, %): 363.2 (M^+, 20), 316.1,[16] 236.1 (100), 121.1,[31] 106.1;[20] LC−MS (negative ion mode): m/z 362.01 $(M-H)^-$ for $C_{20}H_{17}N_3O_4$; Purity (%): 97.23; Tautomeric form (%): 63 Enol.

*4.2.4.8. 5-(2-(4-Bromophenyl)-3-oxoisoindolin-1-yl) Barbituric Acid (**5e**).* Light gray powder; yield: 25%; mp: 260−263 °C; ^{1}H NMR (500 MHz, DMSO-d_6) δ: 11.59 (s, 2H, 2 × NH Keto), 11.07 (s, 2H, 2 × NH Enol), 7.91−6.63 (m, 16H, aromatic), 6.32 (s, 1H, H_a Enol), 6.15 (s, 1H, H_a Keto), 4.09 (s, 1H, H_b Keto); ^{13}C NMR (125 MHz, DMSO-d_6) δ: 188.24, 183.88, 167.38, 163.94, 162.22, 144.90, 144.89, 132.41, 132.38, 132.09, 131.58, 127.93, 126.71, 123.98, 123.05, 122.59, 118.36, 109.75, 83.74, 56.98; MS (m/z, %): 413.1 (M^+, 2), 286,[28] 171 (100), 128.1 (57), 92.1,[47] 65.1 (65), 42.1 (77); LC−MS (negative ion mode): m/z 411.94 $(M-H)^-$ for $C_{18}H_{12}BrN_3O_4$; Purity (%): 96.23; Tautomeric form (%): 57 Enol.

*4.2.4.9. 5-(2-(3,4-Dichlorophenyl)-3-oxoisoindolin-1-yl) Barbituric Acid (**5f**).* Light purple powder; yield: 50%; mp: 238−240 °C; ^{1}H NMR (500 MHz, DMSO-d_6) δ: 11.65 (s, 2H, 2 × NH Keto), 11.12 (s, 2H, 2 × NH Enol), 8.11−7.13 (m, 14H, aromatic), 6.36 (s, 1H, H_a Enol), 6.20 (s, 1H, H_a Keto), 4.15 (s, 1H, H_b Keto); ^{13}C NMR (125 MHz, DMSO-d_6) δ: 184.14, 167.55, 163.42, 161.81, 150.45, 145.89, 138.37, 136.64, 132.92, 132.28, 131.49, 131.27, 131.06, 130.79, 129.80, 128.36, 126.28, 124.57, 124.14, 123.27, 122.74, 121.71, 115.93, 115.38, 85.11, 60.54, 48.25; MS (m/z, %): 403 (M^+, 14), 276 (100), 238,[4] 213,[6] 161;[9] LC−MS (negative ion mode): m/z 401.91 $(M-H)^-$ for $C_{18}H_{11}Cl_2N_3O_4$; Purity (%): 98.32; Tautomeric form (%): 56 Enol.

*4.2.4.10. 5-(3-Oxo-2-(p-tolyl) Isoindolin-1-yl) Barbituric Acid (**5g**).* White powder; yield: 42%; mp: 268−270 °C; ^{1}H NMR (500 MHz, DMSO-d_6) δ: 11.53 (s, 2H, 2 × NH Keto), 11.02 (s, 2H, 2 × NH Enol), 8.01−6.95 (m, 16H, aromatic), 6.31 (s, 1H, H_a Enol), 6.07 (s, 1H, H_a Keto), 4.07 (s, 1H, H_b Keto), 2.41−2.22 (m, 6H, 2 × CH_3 Keto and Enol); ^{13}C NMR (125 MHz, DMSO-d_6) δ: 180.39, 150.71, 135.94, 132.88, 130.60, 129.88, 129.25, 125.12, 122.82, 122.49, 84.45, 61.00, 48.54, 39.83; MS (m/z, %): 349.1 (M^+, 17), 231.1 (64), 222.1 (100), 133.1 (50), 104.1;[42] LC−MS (negative ion mode): m/z 348.01 $(M-H)^-$ for $C_{19}H_{15}N_3O_4$; Purity (%): 97.36; Tautomeric form (%): 44 Enol.

*4.2.4.11. 5-(2-(4-Fluorophenyl)-3-oxoisoindolin-1-yl) Barbituric Acid (**5h**).* White powder; yield: 70%; mp: 270−272 °C; ^{1}H NMR (500 MHz, DMSO-d_6) δ: 11.55 (s, 2H, 2 × NH Keto), 11.07 (s, 2H, 2 × NH Enol), 7.93−6.92 (m, 16H, aromatic), 6.30 (s, 1H, H_a Enol), 6.12 (s, 1H, H_a Keto), 4.08 (s, 1H, H_b Keto); ^{13}C NMR (125 MHz, DMSO-d_6) δ: 164.85, 162.77, 159.30, 157.41, 136.76, 132.94, 127.53, 124.01, 123.95, 122.41, 120.73, 120.66, 116.44, 116.26, 115.13, 82.13, 57.81; MS (m/z, %): 353.1 (M^+, 13), 226.1 (100), 111.1,[23] 84.1;[7] LC−MS (negative ion mode): m/z 351.94 $(M-H)^-$ for $C_{18}H_{12}FN_3O_4$; Purity (%): 98.85; Tautomeric form (%): Enol 68.

*4.2.4.12. 5-(2-(3-Chlorophenyl)-3-oxoisoindolin-1-yl) Barbituric Acid (**5i**).* Light gray powder; yield: 92%; mp: 230−235 °C; ^{1}H NMR (500 MHz, DMSO-d_6) δ: 11.62 (s, 2H, 2 × NH Keto), 11.08 (s, 2H, 2 × NH Enol), 8.05−6.95 (m, 16H), 6.35 (s, 1H, H_a Enol), 6.18 (s, 1H, H_a Keto), 4.10 (s, 1H, H_b Keto); ^{13}C NMR (125 MHz, DMSO-d_6) δ: 167.51, 163.59, 161.98, 159.92, 150.69, 148.40, 146.25, 139.87, 133.89, 132.68, 130.99, 130.43, 128.17, 126.25, 124.11, 123.19, 122.67, 121.68, 120.21, 117.34, 114.94, 114.26, 110.00, 84.66, 60.65, 48.33; MS (m/z, %): 369.1 (M^+, 14), 242.1 (100), 111.1,[13] 75.1;[10] LC−MS

https://doi.org/10.1021/acsomega.2c01028
ACS Omega 2022, 7, 19401−19411

(negative ion mode): m/z 367.97 $(M-H)^-$ for $C_{18}H_{12}ClN_3O_4$; Purity (%): 99.10; Tautomeric form (%): Enol 54.

*4.2.4.13. 5-(2-(3,5-Dichlorophenyl)-3-oxoisoindolin-1-yl) Barbituric Acid (**5j**).* White powder; yield: 50%; mp: 287−290 °C; ^{1}H NMR (500 MHz, DMSO-d_6) δ: 11.69 (s, 2H, 2 × NH Keto), 11.14 (s, 2H, 2 × NH Enol), 8.15−7.20 (m, 14H, aromatic), 6.36 (s, 1H, H_a Enol), 6.23 (s, 1H, H_a Keto), 4.17 (s, 1H, H_b Keto); ^{13}C NMR (125 MHz, DMSO-d_6) δ: 167.71, 163.48, 161.80, 150.40, 145.86, 140.60, 134.79, 134.27, 133.12, 132.12, 129.91, 128.44, 125.70, 123.63, 123.39, 122.78, 119.85, 85.15, 60.45, 48.23; MS (m/z, %): 403.1 (M^+, 18), 276.1 (100), 231.1 (68), 215.1,[26] 133.1 (61), 104.1,[47] 77.1;[33] LC−MS (negative ion mode): m/z 401.91 $(M-H)^-$ for $C_{18}H_{11}Cl_2N_3O_4$; Purity (%): 98.20; Tautomeric form (%): Enol 59.

*4.2.4.14. 5-(2-Isobutyl-3-oxoisoindolin-1-yl) Barbituric Acid (**5k**).* Light yellow powder; yield: 85%; mp: 210−212 °C; ^{1}H NMR (500 MHz, DMSO-d_6) δ: 9.46 (s, 2H, 2 × NH Keto), 9.34 (s, 2H, 2 × NH Enol), 7.84−7.15 (m, 8H, aromatic), 6.60 (s, 1H, H_a Enol), 5.71 (s, 1H, H_a Keto), 3.40 (s, 1H, H_b Keto), 2.71 (d, 2H, CH_2 Keto), 2.56 (d, 2H, CH_2 Enol), 2.03 (m, 1H, CH Keto), 1.77 (m, 1H, CH Enol), 0.88 (d, 6H, 2 × CH_3 Enol), 0.75 (d, 6H, 2 × CH_3 Keto); ^{13}C NMR (125 MHz, DMSO-d6) δ: 171.57, 167.90, 166.10, 164.86, 163.35, 153.03, 152.79, 152.70, 149.33, 133.52, 133.48, 130.67, 127.76, 127.66, 126.59, 124.23, 122.21, 122.08, 80.77, 80.33, 79.66, 78.94, 57.10, 47.01, 46.22, 27.19, 26.80, 21.03, 20.41, 20.11; MS (m/z, %): 315.2 (M^+, 5), 133.1 (57), 83 (100), 42.1;[36] LC−MS (negative ion mode): m/z 314 $(M-H)^-$ for $C_{16}H_{17}N_3O_4$; Purity (%): 98.92; Tautomeric form (%): Enol 71.

*4.2.4.15. 5-(2-Isopropyl-3-oxoisoindolin-1-yl) Barbituric Acid (**5l**).* White powder; yield: 88%; mp: 220−225 °C; ^{1}H NMR (500 MHz, DMSO-d_6) δ: 9.27 (s, 2H, 2 × NH Enol), 7.68 (d, J = 7.5 Hz, 1H, H_4), 7.57 (t, J = 7.5, 1.4 Hz, 1H, H_2), 7.41 (t, J = 7.4 Hz, 1H, H_3), 7.26 (d, J = 7.6 Hz, 1H, H_1), 6.60 (s, 1H, H_a Enol), 3.21 (pd, J = 6.5, 1.8 Hz, 1H, CH), 1.11 (dd, J = 6.6, 1.9 Hz, 6H, 2 × CH_3); ^{13}C NMR (125 MHz, DMSO-d_6) δ: 171.57, 164.91, 153.08, 152.65, 133.47, 127.78, 127.64, 124.23, 122.08, 116.28, 80.66, 80.42, 43.44, 40.48, 40.31, 40.14, 39.97, 39.81, 39.64, 39.47, 20.81; MS (m/z, %): 301.2 (M^+,2), 231.1 (95), 215.1,[32] 133.1 (100), 104.1 (71), 77.1 (49), 44.2 (87); LC−MS (negative ion mode): m/z 299.95 $(M-H)^-$ for $C_{15}H_{15}N_3O_4$; Purity (%): 99.02; Tautomeric form (%): Enol 100.

*4.2.4.16. 1,3-Dimethyl-5-(2-(4-methoxyphenyl)-3-oxoisoindolin-1-yl) Barbituric Acid (**5m**).* Light purple powder; yield: 54%; mp: 140−145 °C; ^{1}H NMR (500 MHz, DMSO-d_6) δ: 7.75 (d, J = 7.5 Hz, 1H, H_4), 7.66 (m, 2H, H_1 and H_2), 7.57 (t, J = 7.4 Hz, 1H, H_3), 7.32 (d, J = 8.5 Hz, 2H, H_6 and H_7), 7.00 (d, J = 8.8 Hz, 2H, H_5 and H_8), 6.09 (d, J = 2.2 Hz, 1H, H_a Keto), 4.30 (d, J = 2.2 Hz, 1H, H_b Keto), 3.77 (s, 3H, OCH_3 Keto), 3.06 (s, 3H, NCH_3 Keto), 2.71 (s, 3H, NCH_3 Keto); ^{13}C NMR (125 MHz, DMSO-d_6) δ: 166.71, 166.56, 165.70, 158.07, 151.10, 143.15, 132.75, 132.35, 129.32, 128.77, 127.22, 123.62, 122.86, 114.61, 62.46, 55.88, 50.17, 28.18; MS (m/z, %): 393.2 (M^+, 19), 238.2 (100), 167.1,[12] 77.1;[5] LC−MS (negative ion mode): m/z 391.7 $(M-H)^-$ for $C_{21}H_{19}N_3O_5$; Purity (%): 98.43; Tautomeric form (%): Enol 0.

*4.2.4.17. 5-(2-(4-Methoxyphenyl)-3-oxoisoindolin-1-yl)-2-thiobarbituric Acid (**5n**).* White powder; yield: 90%; mp: 170−172 °C; ^{1}H NMR (500 MHz, DMSO-d_6) δ: 11.87 (s, 2H, 2 × NH Keto), 11.42 (s, 2H, 2 × NH Enol), 7.93−6.78 (m, 16H, aromatic), 6.47 (s, 1H, H_a Enol), 6.30 (d, J = 1.8 Hz, 1H, H_a Keto), 3.76 (d, J = 1.8 Hz, 1H, H_b Keto), 3.73 (s, 6H, 2 × OCH_3); ^{13}C NMR (125 MHz, DMSO-d_6) δ: 174.26, 167.00, 161.95, 160.25, 159.36, 157.52, 156.65, 145.55, 133.22, 132.09, 131.14, 128.51, 128.11, 124.94, 124.39, 124.24, 122.96, 122.58, 115.36, 114.25, 114.13, 94.97, 89.96, 56.71, 55.92, 55.64, 55.58; MS (m/z, %): 381.2 (M^+, 13), 238.1 (100), 167.1,[18] 144.1,[43] 108.1,[26] 69.1,[17] 45.2;[28] LC−MS (negative ion mode): m/z 379.98 $(M-H)^-$ for $C_{19}H_{15}N_3O_4S$; Purity (%): 99.08; Tautomeric form (%): Enol 13.

4.3. Docking Study. Input files of the ligands and receptor were prepared by AutoDockTools 1.5.7 (ADT).[44] The PDB file of the crystal structure of Jack bean urease with PDB ID: 3LA4 was obtained from http://www.pdb.org and was used as the receptor. The 2D structure of the ligands was drawn by MarvinSketche version 15.2.2. Chem3D ultra version 8.0 converted the 2D structure to the PDB format. The receptor was prepared as follows: all water molecules were deleted, polar hydrogens were added, nonpolar hydrogens were merged, and Kollman charges were assigned. The grid box with the size of 50 × 50 × 50 Å with grid center X = −52.062, Y = −39.851, Z = 82.694, and grid-point spacing of 0.375 Å was located near the Ni atom in the active site of the enzyme. The grid maps of each atom type were calculated using AutoGrid 4.2.[44] Docking simulations were calculated using AutoDock4.2. All parameters of docking simulation were set to default of the software except for the number of running jobs that were set for 30 runs.[18,44,45] Discovery Studio Visualizer (Ver.17.2)[46] and PyMol version 1. Level[47] were used for representing ligand−receptor interactions.

4.4. Urease Inhibition Method. All the chemicals and the reagents were purchased from Merck except for sodium nitroprusside and jack bean urease (EC 3.5.1.5) purchased from Sigma. Deionized water was used for all the experiments. Potassium phosphate buffer (100 mM), pH 7.4, was prepared in distilled water. The method used to examine compounds is the same as the procedures in our previous studies.[18] Thiourea was used as the reference standard inhibitor. The compounds, including **5a−n** and thiourea, were dissolved in deionized water with a maximum of 5% DMSO.

The compounds were tested in a 1 to 100 μg/mL concentration range. Thiourea was used as the standard inhibitor. The assay solution consisted of 850 μL of urea and 100 μL of the test compound. After 30 min of incubation at 37 °C, 35 μL of phosphate buffer (100 mM, pH 7.4) and 15 μL of the urease enzyme were added to the assay solution and again was incubated for 30 min at 37 °C. After the second incubation, 100 μL of each incubated solution was added to the mixture containing 500 μL of phenol reagent (5.0 g of phenol and 25.0 mg of sodium nitroprusside in 500 mL of distilled water) and 500 μL of alkali reagent (containing 2.5 g of sodium hydroxide and 4.2 mL of sodium hypochlorite (5% chlorine) in 500 mL of distilled water). The absorbance of blue indophenols was measured at 625 nm after incubation at 37 °C for 30 min. Thiourea was used as the standard compound, and the uninhibited urease was used as a control.

I (%) = $[1 - (T/C)]$ * 100 equation was used for the calculation of the percentage of enzyme inhibition. I (%) is assigned to the percentage of the inhibition of the enzyme, T is assigned to the absorbance of the tested sample (a mixture including enzyme, enzyme inhibitor, and solvent), and C (control) is assigned to the absorbance of the solvent in the

https://doi.org/10.1021/acsomega.2c01028
ACS Omega 2022, 7, 19401−19411

presence of enzymes without any inhibitor. All the tests were performed in triplicate. All the data are expressed as mean ± standard error mean.[48] The IC_{50} values were calculated using GraphPad Prism 9 software (Graph-Pad Software Inc., San Diego, CA).

■ ASSOCIATED CONTENT

Supporting Information

The Supporting Information is available free of charge at https://pubs.acs.org/doi/10.1021/acsomega.2c01028.

Scans of mass spectra; ^{1}H NMR spectra; ^{13}C NMR spectra; and LC−MS spectra (ZIP)

■ AUTHOR INFORMATION

Corresponding Author

Massoud Amanlou − *Department of Medicinal Chemistry, Faculty of Pharmacy and Experimental Medicine Research Center, Tehran University of Medical Sciences, Tehran 1416634793, Iran;* orcid.org/0000-0002-8559-1668; Phone: +98 21 66959067; Email: amanlou@sina.tums.ac.ir; Fax: +98 21 64121111

Authors

Houman Kazemzadeh − *Department of Medicinal Chemistry, Faculty of Pharmacy, Tehran University of Medical Sciences, Tehran 1416634793, Iran;* orcid.org/0000-0002-3491-0892

Elham Hamidian − *Department of Medicinal Chemistry, Faculty of Pharmacy, Tehran University of Medical Sciences, Tehran 1416634793, Iran*

Faezeh Sadat Hosseini − *Department of Medicinal Chemistry, Faculty of Pharmacy, Tehran University of Medical Sciences, Tehran 1416634793, Iran*

Movahed Abdi − *Department of Medicinal Chemistry, Faculty of Pharmacy, Tehran University of Medical Sciences, Tehran 1416634793, Iran*

Fatemeh Niasari Naslaji − *Department of Medicinal Chemistry, Faculty of Pharmacy, Tehran University of Medical Sciences, Tehran 1416634793, Iran*

Meysam Talebi − *Department of Medicinal Chemistry, Faculty of Pharmacy, Tehran University of Medical Sciences, Tehran 1416634793, Iran*

Mehdi Asadi − *Department of Medicinal Chemistry, Faculty of Pharmacy, Tehran University of Medical Sciences, Tehran 1416634793, Iran*

Mahmood Biglar − *The Institute of Pharmaceutical Sciences (TIPS), Tehran University of Medical Sciences, Tehran 1416634793, Iran*

Issa Zarei − *Department of Medicinal Chemistry, Faculty of Pharmacy, Tehran University of Medical Sciences, Tehran 1416634793, Iran*

Complete contact information is available at: https://pubs.acs.org/10.1021/acsomega.2c01028

Notes

The authors declare no competing financial interest.

■ ACKNOWLEDGMENTS

This research was funded by the Tehran University of Medical Sciences and Health Services.

■ REFERENCES

(1) Wroblewski, L. E.; Peek, R. M., Jr.; Wilson, K. T. *Helicobacter pylori* and gastric cancer: factors that modulate disease risk. *Clin. Microbiol. Rev.* **2010**, *23*, 713−739.

(2) Yusefi, A. R.; Lankarani, K. B.; Bastani, P.; Radinmanesh, M.; Kavosi, Z. Risk factors for gastric cancer: a systematic review. *Asian Pac. J. Cancer Prev.* **2018**, *19*, 591.

(3) Uemura, N.; Okamoto, S.; Yamamoto, S.; Matsumura, N.; Yamaguchi, S.; Yamakido, M.; Taniyama, K.; Sasaki, N.; Schlemper, R. J. *Helicobacter pylori* infection and the development of gastric cancer. *N. Engl. J. Med.* **2001**, *345*, 784−789.

(4) Traulsen, J.; Zagami, C.; Daddi, A. A.; Boccellato, F. Molecular modelling of the gastric barrier response, from infection to carcinogenesis. *Best Pract. Res., Clin. Gastroenterol.* **2021**, *50*−*51*, No. 101737.

(5) Fiori-Duarte, A. T.; Rodrigues, R. P.; Kitagawa, R. R.; Kawano, D. F. Insights into the Design of Inhibitors of the Urease Enzyme-A Major Target for the Treatment of *Helicobacter pylori* Infections. *Curr. Med. Chem.* **2020**, *27*, 3967−3982.

(6) Hameed, A.; Al-Rashida, M.; Uroos, M.; Qazi, S. U.; Naz, S.; Ishtiaq, M.; Khan, K. M. A patent update on therapeutic applications of urease inhibitors (2012−2018). *Expert Opin. Ther. Pat.* **2019**, *29*, 181−189.

(7) El-Deeb, N.; Al-Madboly, L. Probiotics and GIT diseases/stomach ulcer. *Probiotics, Nat Microbiota in Living Org Fundam Appl.*; CRC Press, 2021.

(8) Roberts-Thomson, I. C. How did the ancient bacterium, *Helicobacter pylori*, cause an epidemic of chronic duodenal ulceration? *JGH Open* **2021**, *5*, 636.

(9) Debraekeleer, A.; Remaut, H. Future perspective for potential *Helicobacter pylori* eradication therapies. *Future Microbiol.* **2018**, *13*, 671−687.

(10) Hassan, S. T.; Švajdlenka, E. Biological evaluation and molecular docking of protocatechuic acid from *Hibiscus sabdariffa* L. as a potent urease inhibitor by an ESI-MS based method. *Molecules* **2017**, *22*, 1696.

(11) Sedaghati, S.; Azizian, H.; Montazer, M. N.; Mohammadi-Khanaposhtani, M.; Asadi, M.; Moradkhani, F.; Ardestani, M. S.; Asgari, M. S.; Yahya-Meymandi, A.; Biglar, M. Novel (thio) barbituric-phenoxy-N-phenylacetamide derivatives as potent urease inhibitors: synthesis, in vitro urease inhibition, and in silico evaluations. *Struct. Chem.* **2021**, *32*, 37−48.

(12) Asgari, M. S.; Azizian, H.; Nazari Montazer, M.; Mohammadi-Khanaposhtani, M.; Asadi, M.; Sepehri, S.; Ranjbar, P. R.; Rahimi, R.; Biglar, M.; Larijani, B. New 1, 2, 3-triazole−(thio) barbituric acid hybrids as urease inhibitors: design, synthesis, in vitro urease inhibition, docking study, and molecular dynamic simulation. *Arch. Pharm.* **2020**, *353*, No. 2000023.

(13) Pedrood, K.; Azizian, H.; Montazer, M. N.; Mohammadi-Khanaposhtani, M.; Asgari, M. S.; Asadi, M.; Bahadorikhalili, S.; Rastegar, H.; Larijani, B.; Amanlou, M. Arylmethylene hydrazine derivatives containing 1, 3-dimethylbarbituric moiety as novel urease inhibitors. *Sci. Rep.* **2021**, *11*, 1−16.

(14) Tomlin, S. L.; Jenkins, A.; Lieb, W. R.; Franks, N. P. Preparation of barbiturate optical isomers and their effects on GABA (A) receptors. *J. Am. Soc. Anesthesiol.* **1999**, *90*, 1714−1722.

(15) Peytam, F.; Adib, M.; Mahernia, S.; Rahmanian-Jazi, M.; Jahani, M.; Masoudi, B.; Mahdavi, M.; Amanlou, M. Isoindolin-1-one derivatives as urease inhibitors: Design, synthesis, biological evaluation, molecular docking and in-silico ADME evaluation. *Bioorg. Chem.* **2019**, *87*, 1−11.

(16) Jia, P.; Pei, J.; Wang, G.; Pan, X.; Zhu, Y.; Wu, Y.; Ouyang, L. The roles of computer-aided drug synthesis in drug development. *Green Synth. Catal.* **2021**, *3*, 11.

(17) Gurung, A. B.; Ali, M. A.; Lee, J.; Farah, M. A.; Al-Anazi, K. M. An Updated Review of Computer-Aided Drug Design and Its Application to COVID-19. *BioMed Res. Int.* **2021**, *2021*, No. 8853056.

(18) Azizian, H.; Nabati, F.; Sharifi, A.; Siavoshi, F.; Mahdavi, M.; Amanlou, M. Large-scale virtual screening for the identification of

new *Helicobacter pylori* urease inhibitor scaffolds. *J. Mol. Model.* **2012**, *18*, 2917−2927.
(19) Nazari Montazer, M.; Asadi, M.; Bahadorikhalili, S.; Hosseini, F. S.; Amanlou, A.; Biglar, M.; Amanlou, M. Design, synthesis, docking study and urease inhibitory activity evaluation of novel 2-((5-amino-1, 3, 4-thiadiazol-2-yl) thio)-N-arylacetamide derivatives. *Med. Chem. Res.* **2021**, *30*, 729−742.
(20) Biglar, M.; Mirzazadeh, R.; Asadi, M.; Sepehri, S.; Valizadeh, Y.; Sarrafi, Y.; Amanlou, M.; Larijani, B.; Mohammadi-Khanaposhtani, M.; Mahdavi, M.; Novel, N. N-dimethylbarbituric-pyridinium derivatives as potent urease inhibitors: Synthesis, in vitro, and in silico studies. *Bioorg. Chem.* **2020**, *95*, No. 103529.
(21) Upadhyay, S. P.; Thapa, P.; Sharma, R.; Sharma, M. 1-Isoindolinone scaffold-based natural products with a promising diverse bioactivity. *Fitoterapia* **2020**, *146*, No. 104722.
(22) Khan, K. M.; Ali, M.; Wadood, A.; Khan, M.; Lodhi, M. A.; Perveen, S.; Choudhary, M. I.; Voelter, W. Molecular modeling-based antioxidant arylidene barbiturates as urease inhibitors. *J. Mol. Graphics Modell.* **2011**, *30*, 153−156.
(23) Bano, B.; Khan, K. M.; Begum, F.; Lodhi, M. A.; Salar, U.; Khalil, R.; Ul-Haq, Z.; Perveen, S. Benzylidine indane-1, 3-diones: As novel urease inhibitors; synthesis, in vitro, and in silico studies. *Bioorg. Chem.* **2018**, *81*, 658−671.
(24) Krasnov, K.; Kartsev, V.; Santarovich, E. Reaction of Barbituric, 2-Thiobarbituric Acids and Their Derivatives with 2-Carboxybenzaldehyde and Opianic Acid: Synthesis and Tautomerism of 5-(3′-Oxo-1′, 3′-dihydroisobenzofuran-1′-yl) barbituric Acids and Their 2-Thio Analogs. *Chem. Heterocycl. Compd.* **2002**, *38*, 702−709.
(25) Motamedi, A.; Sattari, E.; Mirzaei, P.; Armaghan, M.; Bazgir, A. An efficient and green synthesis of phthalide-fused pyrazole and pyrimidine derivatives. *Tetrahedron Lett.* **2014**, *55*, 2366−2368.
(26) Huang, S.-Y.; Zou, X. Advances and challenges in protein-ligand docking. *Int. J. Mol. Sci.* **2010**, *11*, 3016−3034.
(27) Chen, Y.-C. Beware of docking! *Trends Pharmacol. Sci.* **2015**, *36*, 78−95.
(28) Mikra, C.; Rossos, G.; Hadjikakou, S.; Kourkoumelis, N. Molecular Docking and Structure Activity Relationship Studies of NSAIDs. What do they Reveal about IC50? *Lett. Drug Des. Discovery* **2017**, *14*, 949−958.
(29) Daina, A.; Michielin, O.; Zoete, V. SwissADME: a free web tool to evaluate pharmacokinetics, drug-likeness and medicinal chemistry friendliness of small molecules. *Sci. Rep.* **2017**, *7*, 42717.
(30) Delaney, J. S. ESOL: estimating aqueous solubility directly from molecular structure. *J. Chem. Inf. Comput. Sci.* **2004**, *44*, 1000−1005.
(31) Bojarski, J. T.; Mokrosz, J. L.; Bartoń, H. J.; Paluchowska, M. H. Recent progress in barbituric acid chemistry. *Adv. Heterocycl. Chem.* **1985**, *38*, 229−297.
(32) Jovanovic, M. V.; Biehl, E. R. Substituent and solvent effects on tautomeric equilibria of barbituric acid derivatives and isosterically related compounds. *J. Heterocycl. Chem.* **1987**, *24*, 191−204.
(33) Neiland, O. Y.; Stradyn, Y. P.; Silin'sh, E.; Balone, R.; Valter, S.; Kadysh, V.; Kalnin', S.; Kampar, V.; Mazheika, I.; Taure, L. *Structure and Tautomeric Transformations of β-Dicarbonyl Compounds*; Zinatne: Riga, 1977; p 52.
(34) Kabachnik, M.; Yoffe, S.; Vatsuro, K. Tautomeric equilibrium of ketonic and cis-and trans-enolic forms of β-dicarbonyl compounds in solution. *Tetrahedron* **1957**, *1*, 317−327.
(35) Laurella, S, Colasurdo, D, Ruiz, D, Allegretti, P. NMR as a Tool for Studying Rapid Equilibria: Tautomerism. In *Applications of NMR Spectroscopy*; Bentham, 2017; Vol. *6*, pp 1−46.
(36) Żuchowski, G.; Zborowski, K. The influence of solvent molecules on NMR spectrum of barbituric acid in the DMSO solution. *Cent. Eur. J. Chem.* **2006**, *4*, 523−532.
(37) Reeves, L. Nuclear magnetic resonance measurements in solutions of acetylacetone: the effect of solvent interactions on the tautomeric equilibrium. *Can. J. Chem.* **1957**, *35*, 1351−1365.
(38) Claramunt, R.; López, C.; Santa María, M.; Sanz, D.; Elguero, J. The use of NMR spectroscopy to study tautomerism. *Prog. Nucl. Magn. Reson. Spectrosc.* **2006**, *49*, 169−206.
(39) Best, D.; Burns, D. J.; Lam, H. W. Direct Synthesis of 5-Aryl Barbituric Acids by Rhodium (II)-Catalyzed Reactions of Arenes with Diazo Compounds. *Angew. Chem., Int. Ed.* **2015**, *127*, 7518−7521.
(40) Bhattacharjee, D.; Sheet, S. K.; Khatua, S.; Biswas, K.; Joshi, S.; Myrboh, B. A reusable magnetic nickel nanoparticle based catalyst for the aqueous synthesis of diverse heterocycles and their evaluation as potential anti-bacterial agent. *Biorg. Med. Chem.* **2018**, *26*, 5018−5028.
(41) Kalita, S. J.; Deka, D. C. 2-Phenyl-2, 3-dihydrobenzo [d] thiazole: A Mild, Efficient, And Highly Active In Situ Generated Chemoselective Reducing Agent For The One-Pot Synthesis Of 5-Monoalkylbarbiturates in Water. *Synlett* **2018**, *29*, 477−482.
(42) Katritzky, A. R.; Hall, C. D.; El-Gendy, B. E.-D. M.; Draghici, B. Tautomerism in drug discovery. *J. Comput.-Aided Mol. Des.* **2010**, *24*, 475−484.
(43) Allen, G.; Dwek, R. A. An nmr study of keto−enol tautomerism in β-diketones. *J. Chem. Soc. B* **1966**, 161−163.
(44) Morris, G. M.; Huey, R.; Lindstrom, W.; Sanner, M. F.; Belew, R. K.; Goodsell, D. S.; Olson, A. J. AutoDock4 and AutoDockTools4: Automated docking with selective receptor flexibility. *J. Comput. Chem.* **2009**, *30*, 2785−2791.
(45) Hosseini, F. S.; Amanlou, M. Anti-HCV and anti-malaria agent, potential candidates to repurpose for coronavirus infection: virtual screening, molecular docking, and molecular dynamics simulation study. *Life Sci.* **2020**, *258*, No. 118205.
(46) Dassault Systèmes BIOVIA, Discovery Studio Modeling Environment, Release 2017, San Diego: Dassault Systèmes, 2016, Version 17.2 [software], Available from: https://www.3dsbiovia.com/products/collaborative-science/biovia-discovery-studio.
(47) The PyMOL molecular graphics system, Version 1. level, Schrodinger LLC, Available from: https://pymol.org.
(48) Atay, I.; Kirmizibekmez, H.; Kaiser, M.; Akaydin, G.; Yesilada, E.; Tasdemir, D. Evaluation of in vitro antiprotozoal activity of Ajuga laxmannii and its secondary metabolites. *Pharm. Biol.* **2016**, *54*, 1808−1814.

https://doi.org/10.1021/acsomega.2c01028
ACS Omega 2022, 7, 19401−19411